Preprints of the 7th IFAC Symposium on Advances in Automotive Control, National Olympics Memorial Youth Center, Tokyo, Japan, September 4-7, 2013

Basic Design of Electric Vehicle Motion Control System Using Single Antenna GPS Receiver

Binh Minh Nguyen* Alexander Viehweider* Hiroshi Fujimoto* Yoichi Hori*

**Department of Advanced Energy, the University of Tokyo, Japan,*
(e-mail: minh@hori.k.u-tokyo.ac.jp, hori@k.u-tokyo.ac.jp, fujimoto@k.u-tokyo.ac.jp).

Abstract: By integrating a single antenna GPS receiver and dynamic sensors, key states for electric vehicle motion control system can be estimated, including yaw angle, sideslip angle, longitudinal velocity, and lateral velocity. In order to achieve accurate state estimation, Kalman filter with disturbance accommodating technique considering the handling of time delay in measurements using GPS is proposed. In this paper, three motion controls of electric vehicle based on the estimated states are demonstrated. The first is attitude control using front steering angle with feedback-feedforward controller and disturbance observer. The second is a traction control based on wheel slip ratio control system using sliding mode control theory. The last is lateral stability control using estimated sideslip angle.

Keywords: electric vehicles, global positioning system, Kalman filter, state estimation, motion control.

1. INTRODUCTION

Electric vehicles (EVs) became a novel motion control systems, thanks to the remarkable advantages of electric motors (Hori, 2004). The big issue in motion control design is how to precisely obtain the key vehicle states in real time. Various states are required to be known for different control purpose: sideslip angle for lateral stability control, longitudinal velocity for wheel slip ratio control, yaw angle for attitude control of electric vehicle, etc. The fact is that reliable sensors to measure such kind of motion information are unavailable at affordable cost. For instance, Corrsys-Datron produced the noncontact optical sensor for accurately measuring both longitudinal velocity and sideslip angle. However, due to the very high cost, it cannot be a practical solution for commercial vehicles.

Vehicle state estimation using on-board dynamic sensors have been widely researched (Aoki *et al.*, 2005) (Chen *et al.*, 2008) (Zhao *et al.*, 2011) and applied in motion control of vehicle (Chung *et al.*, 2006) (Geng *et al.*, 2009). However, the measurements of dynamic sensor such as gyroscope and accelerometers are often influenced by strong noise, bias, gravity on bank road, and the wind effect is also not properly captured. The variation of estimation model's parameters like cornering stiffness according to road condition is another problem in state estimation of vehicle.

Since the last decade, global positioning system (GPS) has been a candidate for vehicle state estimation. Besides the absolute position of vehicle, GPS receiver can provide other motion measurement that cannot be obtained from conventional dynamic sensor. They are velocity and attitude angle or course angle of vehicle. By using double antenna GPS receiver, sideslip angle can be calculated directly without vehicle model (Bevly *et al.*, 2006). This method was applied in vehicle stability control system (Daily *et al.*, 2004). However, the main disadvantage of this method is the poor update rate of GPS receiver which is often less than 50 Hz. Thus, this method is not applicable for advanced motion control of EV in which the actuators (in-wheel motors or EPS motors) can be manipulated at high frequency of 1 kHz or more. In order to provide high rate estimation, the fusion of GPS receiver with dynamic sensor has been studied. For instance, the combination of single antenna GPS receiver with gyroscope (Anderson *et al.*, 2004) or magnetometer

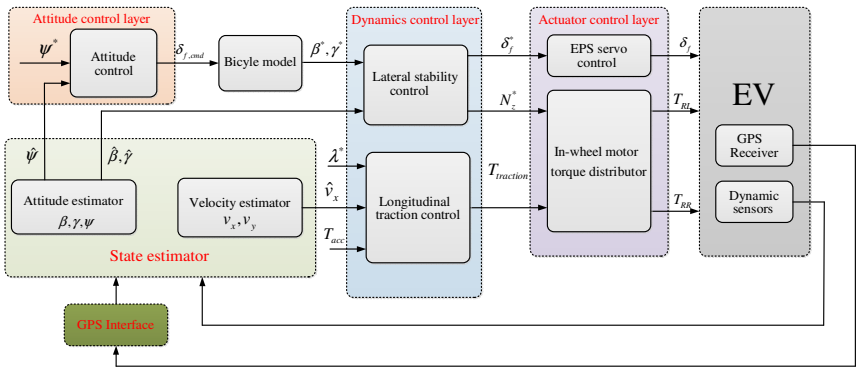

Fig. 1. EV motion control system using the integration of single antenna GPS receiver and dynamic sensors.

(Yoon *et al.*, 2012) was proposed for sideslip angle estimation. In these methods, the robustness of estimation under model uncertainties and external disturbances were not deeply examined. Moreover, time delay of data transfer from GPS receiver challenges the accuracy of state estimation. Using two single antenna GPS receivers, the yaw angle is calculated directly (Yoon *et al.*, 2010). Then, sideslip angle is estimated based on the fusion of this calculated yaw angle with data from inertial measurement unit (IMU). Needless to say, this method increases the cost of the estimation system. Moreover, technically speaking, it is a nontrivial work to synchronize the data from two GPS receivers into the control system.

We propose the state estimator for EV using the integration of single antenna GPS receiver and dynamic sensors. The estimator consists of two layers and can provide the key states for EV motion control: sideslip angle, yaw angle, longitudinal velocity, and lateral velocity. In the past publication, we examined Kalman filter algorithm considering the enhancement of estimation between two consecutive updates of GPS data (Nguyen *et al.*, 2013b). In this paper, state estimator using Kalman filter with disturbance estimation considering the time delay of GPS is proposed. Based on the state estimator, a framework of EV motion control is designed as in Fig. 1. Three local motion controls are demonstrated in this paper. The first is attitude control using front steering angle. The second is a traction system based on wheel slip ratio control in which the controller is designed using sliding mode theory. The last is lateral stability control using the estimated sideslip angle.

2. EXPERIMENTAL SETUP AND MODELING

2.1 Experimental Setup

A one seat micro EV is used for this research (Fig. 2) with two rear in-wheel motors and front EPS system which is applicable for steer-by-wire mode. Optical sensor produced by Corrsys-Datron is installed in the EV to measure the sideslip angle, longitudinal velocity, and lateral velocity for comparing with the estimated values. Dynamic sensors including gyroscope and accelerometers are installed at the center of gravity of the EV. Encoders are used for obtaining the rotational velocity of in-wheel motors and the steering angle. Vehicle control unit (VCU) with RT-Linux operating system is used to implement the estimation and control algorithm. The basic sampling time of the system is 1 millisecond which is the same as that of dynamic sensors. A real-time-kinematic (RTK) GPS receiver, the Hemisphere R320 OmniSTAR, is used to measure the position of vehicle with the accuracy level of 1 centimeter RMS at 20 Hz update rate. From the measurement of position, vehicle velocity and course angle are obtained in real-time.

2.2 Modeling of Experimental EV

To estimate yaw angle, planar bicycle model is used (Fig. 3) to establish the following state space equation:

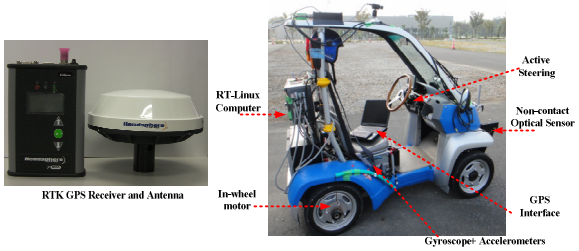

Fig. 2. Experimental EV and GPS receiver

Table 1. Nomenclatures.

Planar bicycle model (lateral motion)	
β	Sideslip angle
V	Velocity vector
v_x, v_y	Longitudinal and lateral velocity
a_x, a_y	Longitudinal and lateral acceleration
γ, ψ, ν	Yaw rate, yaw angle, and course angle
δ_f	Front steer angle
N_z	Yaw moment
C_f, C_r	Front and rear tire cornering stiffness
I_z	Yaw moment of inertia
M	Total mass of vehicle
l_f, l_r	Distance from front and rear axle to CG
F_{yf}, F_{yr}	Front and rear lateral force
On-wheel model (longitudinal motion)	
F_d	Driving force at tire-road contact path
F_r	Driving force at tire-road contact path
T_m	Motor torque
r	Wheel radius
I_ω	Wheel moment of inertia
λ	Wheel slip ratio

$$\begin{cases} \dot{x}_1 = A_1 x_1 + B_1 u_1 \\ y_1 = C_1 x_1 \end{cases} \tag{1}$$

$$x_1 = \begin{bmatrix} \beta & \gamma & \psi \end{bmatrix}^T, u_1 = \begin{bmatrix} \delta_f & N_z \end{bmatrix}^T, y_1 = \begin{bmatrix} \gamma & \nu \end{bmatrix} \tag{2}$$

$$A_1 = \begin{bmatrix} \dfrac{-2(C_f + C_r)}{Mv_x} & -1 - \dfrac{2(C_f l_f - C_r l_r)}{Mv_x^2} & 0 \\ \dfrac{-2(C_f l_f - C_r l_r)}{I_z} & \dfrac{-2(C_f l_f^2 + C_r l_r^2)}{I_z v_x} & 0 \\ 0 & 1 & 0 \end{bmatrix} \tag{3}$$

$$B_1 = \begin{bmatrix} \dfrac{2C_f}{Mv_x} & 0 \\ \dfrac{2C_f l_f}{I_z} & \dfrac{1}{I_z} \\ 0 & 0 \end{bmatrix}, \quad C_1 = \begin{bmatrix} 0 & 1 & 0 \\ 1 & 0 & 1 \end{bmatrix}$$

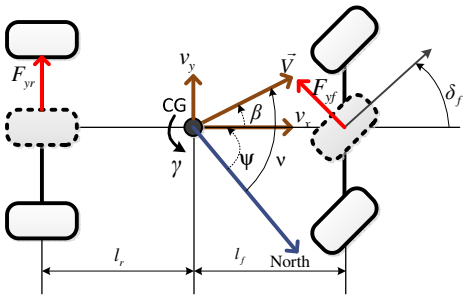

Fig. 3. Planar bicycle model of electric vehicle.

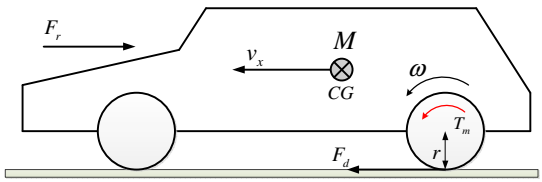

Fig. 4. Longitudinal motion model of electric vehicle.

In planar bicycle model, course angle from GPS receiver is the angle between velocity vector and the geodetic North direction, and it equals to yaw angle plus sideslip angle. The lateral and longitudinal can be calculated from velocity vector (obtained from GPS) and sideslip angle as follows:

$$\tilde{v}_x = V\cos\beta,\ \tilde{v}_y = V\sin\beta \tag{4}$$

To estimate the longitudinal and lateral velocity at high rate, the following state space model is constructed:

$$\begin{cases} \dot{x}_2 = A_2 x_2 + B_2 u_2 \\ y_2 = C_2 x_2 \end{cases} \tag{5}$$

$$x_2 = \begin{bmatrix} v_x & v_y \end{bmatrix},\ u_2 = \begin{bmatrix} a_x & a_y \end{bmatrix}^T,\ y_2 = \begin{bmatrix} \tilde{v}_x & \tilde{v}_y \end{bmatrix} \tag{6}$$

$$A_2 = \begin{bmatrix} 0 & \gamma \\ -\gamma & 0 \end{bmatrix},\ B_2 = \begin{bmatrix} 1 & 0 \\ 0 & 1 \end{bmatrix},\ C_2 = \begin{bmatrix} 1 & 0 \\ 0 & 1 \end{bmatrix} \tag{7}$$

For the sake of simplicity, on-wheel model is used for traction control design of EV (Fig. 4). Considering the acceleration case, the longitudinal motion is expressed as:

$$I_\omega \dot{\omega} = T_m - rF_d \tag{8}$$

$$M\dot{v}_x = F_d - F_r \tag{9}$$

$$\lambda = \frac{r\omega - v_x}{r\omega} \tag{10}$$

3. VEHICLE STATE ESTIMATION DESIGN

3.1 Disturbance Accommodating Estimation Model

In conventional Kalman filter algorithm, the model is often constructed using the nominal parameters. Therefore, the accuracy of estimation may be degraded due to model uncertainties and external disturbances. Disturbance accommodating is a simple but effective method to solve this problem. As the first publication, the unknown disturbance terms can be augmented to be extended states in a control system based on LQR theory (Johnson, 1971). This idea was applied in Kalman filter design for sideslip angle estimation using GPS (Nguyen *et al.*, 2013a). The unknown disturbance terms are assumed to be random walk processes. By selecting the suitable rates of random walks and the process and measurement noise covariance matrices, the unknown terms can be estimated. This means the accuracy of state estimation using Kalman filter is enhanced.

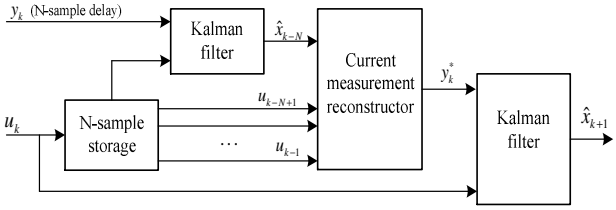

Fig. 5. Kalman filter with reconstruction of measurement in present time.

3.2 Reconstruction of Present Time Measurement

Time delays consisting of few samples can be handled in Kalman filter algorithm by augmenting the state vector accordingly (Hsiao *et al.*, 1996). However, if the delay stands for a big number of samples, the size of the augmented state space system will increase considerably. Larsen proposed a well-known method based on the extrapolating the measurement to present time (Larsen *et al.*, 1998). In this method, the size of Kalman filter is unchanged, burden in Kalman gain calculation. In this paper, the present time measurement is reconstructed from the delayed measurement and the control input stored in an N-step-storage.

A system with N-sample delay measurement is expressed as follows:

$$\begin{cases} x_{k+1} = A_n x_k + B_n u_k \\ y_k = C_n x_{k-N} \end{cases} \tag{11}$$

When the delayed measurement comes, it can be used to estimate the state at N samples before $\hat{x}_{k-N}$. Using this estimate, the measurement at present time can be constructed as follows:

$$\begin{cases} x^*_{k-N+1} = A_d \hat{x}_{k-N} + B_d u_{k-N} \\ x^*_{k-N+2} = A_d x^*_{k-N+1} + B_d u_{k-N+1} \\ \cdots \\ x^*_k = A_d x^*_{k-1} + B_d u_{k-1} \\ y^*_k = C_d x^*_k \end{cases} \tag{12}$$

Block diagram of Kalman filter with present time measurement reconstruction is shown in Fig. 5. The general formulation of the reconstruction is expressed as follows:

$$y^*_k = C_d \left(A_d^N \hat{x}_{k-N} + \sum_{j=1}^{N} A_d^{N-j} B_d u_{k-N+j-1} \right) \tag{13}$$

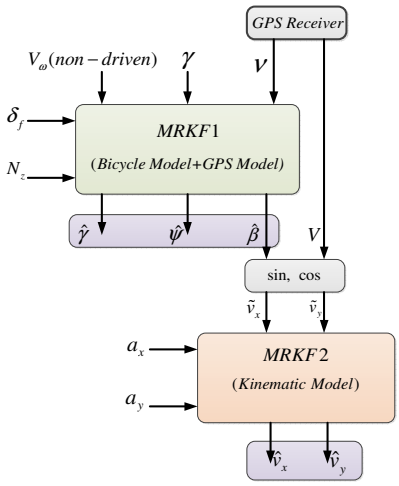

Fig. 6. Double-layer state estimator of EV.

3.3 Vehicle State Estimator

Two models established in section 2 are used for constructing the double-layer state estimator of EV (Fig. 6). Each layer is designed using the disturbance accommodating method with the reconstruction of GPS measurements in present time. The detailed Kalman filter algorithm can be found in the previous publication of our group (Nguyen *et al.*, 2013a, b).

As expressed in (1)-(3), the model of the first layer is used for estimating yaw angle and sideslip angle. This model utilizes the fusion of course angle obtained from GPS receiver and yaw rate measured by gyroscope. In this model, velocity is a time varying parameter instead of vehicle state. Therefore, it is reasonable to use the velocity of non-driven wheel as the approximate measurement of longitudinal velocity.

Thanks to the estimated sideslip angle from the fist layer and measured velocity vector from GPS receiver, longitudinal and lateral velocity can be obtained using (4) but at low update rate. In order to achieve velocity estimation at high rate, accelerometers and gyroscope are used to establish the second layer model as (5)-(7).

4. MOTION CONTROL DESIGN

4.1 Attitude Control Design

Attitude control is one important function in motion control system. In recent year, attitude control considering lateral dynamic has been proposed (Suzuki, 2012). However, in this method, yaw angle is obtained from only IMU which is influenced by strong noise or bias. Moreover, only PID controller is designed to track the yaw angle of vehicle with the reference value. From the planar bicycle model, the transfer function from front steering angle to yaw angle is established as:

$$P_{\delta_f \to \psi}(s) = \frac{\psi(s)}{\delta_f(s)} = \frac{n_1 s + n_0}{s^3 + d_2 s^2 + d_1 s} \tag{14}$$

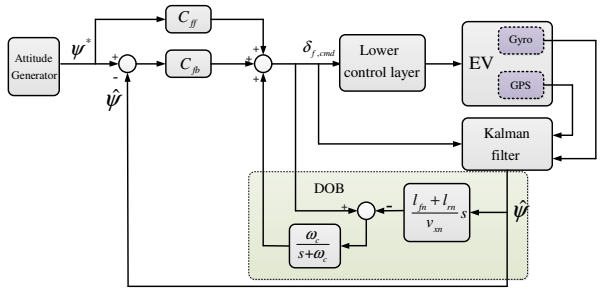

Fig. 7. Robust yaw angle control based on DOB.

In (14), n_1, n_0, d_2, and d_1 are calculated from vehicle model parameter, such as cornering stiffness, yaw moment of initial… with longitudinal velocity. In fact, the values of cornering stiffness can change according to road condition. Therefore, the transfer function from front steering angle to yaw angle contains time-varying parameters. PID controller with constant gains cannot assure the robustness of yaw angle control under the change of road condition and the influence of external disturbances like lateral wind force or gravity on bank road.

Disturbance observer (DOB) was firstly introduced by Ohnishi and then further refined by Hori's group (Ohnishi, 1987) (Umeno and Hori, 1991). According to this method, the feedback loop includes a model of the dynamic of the exogenous reference and disturbance signal, called nominal internal model. By carefully designing the nominal model and a Q-filter, the perfect asymptotic tracking and disturbance compensation are achieved. Until now, DOB has been widely applied in robust motion control, including motion control of EV, such as lateral force observer and yaw moment observer (Fujimoto and Yamauchi, 2010).

To improve the robustness of yaw angle control system using front steering angle, the nominal internal model is designed as followings:

$$P_{(\delta_f \to \psi)n}(s) = \frac{v_{xn}}{(l_{fn} + l_m)s} \tag{15}$$

The nominal model is proposed under the assumption that velocity does not change quickly, sideslip angle and front steering angle are small. We proposed a novel yaw angle control system with disturbance observer as shown in Fig. 7. In this control system, yaw angle is estimated using the first layer of the state estimator designed in section 3. The following low-pass-filter is designed to assure the internal stability. To track the real yaw angle with the reference values, feedback and feedforward controllers are utilized. The feedforward controller is designed by inversing the nominal model in (15) while the feedback controller is designed as PI law using pole placement method.

4.2 Wheel Slip Ratio Control Design

From (8)-(10), a dynamic model for wheel slip ratio control is established as follows:

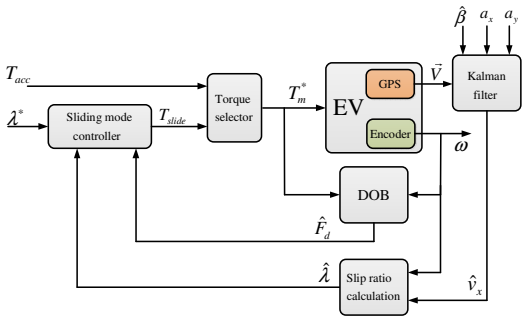

Fig. 8. Wheel slip ratio control based on sliding mode control and DOB.

$$\dot{\lambda} = -\frac{\dot{v}_x}{v_x}\lambda + \frac{v_x}{I_\omega r\omega^2}T_m - \frac{\dot{v}_x}{v_x} - \frac{v_x}{I_\omega\omega^2}F_d \tag{16}$$

Thanks to the in-wheel motor, driving force F_d can be estimated easily from disturbance observer (DOB) using motor torque and wheel velocity (Furukawa and Hori, 2003). The slip ratio is obtained from estimated longitudinal velocity and wheel velocity. Sliding model theory is applied to design the wheel slip ratio controller. The sliding surface, reaching law, and Lyapunov function V are expressed as follows:

$$S = \left(\lambda - \lambda^*\right) \tag{17}$$

$$\dot{S} = -LS - Qsat(S) \tag{18}$$

$$V = \frac{1}{2}S^2 \tag{19}$$

$$\dot{V} = S\dot{S} = -LS^2 - QSsat(S) \tag{20}$$

In (18), L and Q are selected as positive constant. Thus, $\dot{V}$ is always negative. In other words, the stability of the control system is confirmed. A sliding mode control law is obtained as follows with the estimated slip ratio and the observation of driving force:

$$T_{slide} = \frac{I_\omega r\omega^2}{\hat{v}_x}\left[\frac{\dot{\hat{v}}_x}{\hat{v}_x}(1-\lambda) + \dot{\lambda}^* + \frac{\hat{v}_x}{I_\omega\omega^2}\hat{F}_d - LS - Qsat(S)\right] \tag{21}$$

The wheel slip ratio control system is shown in Fig. 8.

4.3 Lateral Stability Control Design

Using the bicycle model, lateral motion of vehicle can be expressed as follows:

$$\begin{bmatrix}\dot{\beta}\\ \dot{\gamma}\end{bmatrix} = \begin{bmatrix}a_{n11} & a_{n12}\\ a_{n21} & a_{n22}\end{bmatrix}\begin{bmatrix}\beta\\ \gamma\end{bmatrix} + \begin{bmatrix}b_{n11} & b_{n12}\\ b_{n21} & b_{n22}\end{bmatrix}\begin{bmatrix}\delta_f\\ N_z\end{bmatrix} + \begin{bmatrix}d_1\\ d_2\end{bmatrix} \tag{22}$$

In (22), the disturbance terms d_1 and d_2 represent the influences of external disturbances and the variation of vehicle parameters from the nominal values. By the Kalman filter with disturbance accommodating methods (the first layer of state estimator), not only sideslip angle but also the disturbance terms can be estimated. Using the disturbance

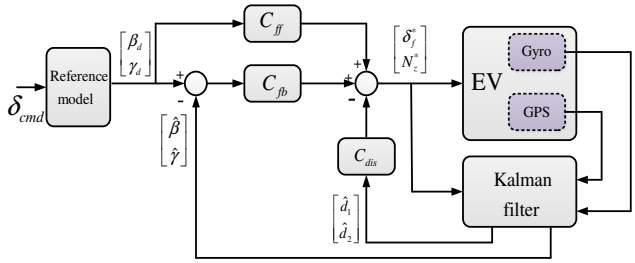

Fig. 9. Lateral stability control system of EV with disturbance accommodating in Kalman filter.

accommodating Kalman filter, we propose lateral stability control system which is the combination of feedback-feed forward controller and the disturbance rejection (Fig. 9). Front steering angle and yaw moment are selected as the control inputs for controlling both the yaw rate and the sideslip angle.

The reference values of sideslip angle and yaw rate are calculated as the steady state responses from the driver's steering angle command. The feed forward controller is designed by inversing model (22) with zero disturbances. Model following method is applied to design the feedback controller. The desired model is designed as follows:

$$\begin{bmatrix}\beta\\ \gamma\end{bmatrix} = \begin{bmatrix}\dfrac{K_\beta}{s+K_\beta} & 0\\ 0 & \dfrac{K_\gamma}{s+K_\gamma}\end{bmatrix}\begin{bmatrix}\beta^*\\ \gamma^*\end{bmatrix} \tag{23}$$

In (23), the cut-off frequencies K_β and K_γ are determined by trial and error experiments to ensure the best responsibility of the sideslip angle and the yaw rate in the respect of steering angle command.

In order to nominalize the system and enhance the robustness of lateral stability control, we have to compensate d_1 and d_2 which represents the total influence of disturbances and model uncertainties must be compensated. The disturbance rejection matrix is designed as follows:

$$C_{dis} = \begin{bmatrix}b_{n11} & b_{n12}\\ b_{n21} & b_{n22}\end{bmatrix}^{-1} \tag{24}$$

5. EXPERIMENTAL VERIFICATION

5.1 Verification of Double Layer State Estimator

In order to simulate the conventional GPS receiver, measurements from Hemisphere R320 are sampled at 200 milliseconds (or 5 Hz update rate) and the time delay is set as 100 milliseconds.

Results of sideslip angle estimation are shown in Fig. 10 (a). Another sideslip angle estimation method using dynamic sensors is performed for comparison. This method was proposed based on linear observer using the measurement of

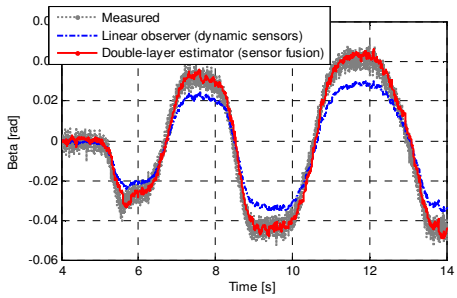

(a) Sideslip angle estimation results.

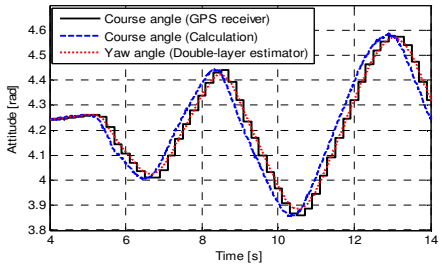

(b) Yaw angle estimation results.

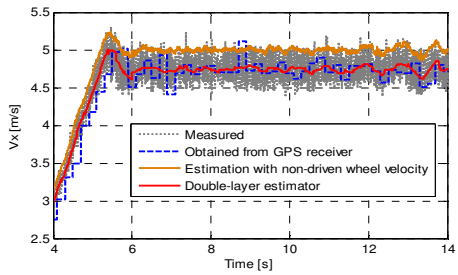

(c) Longitudinal velocity estimation results.

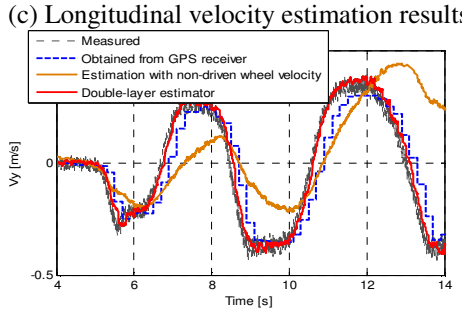

(d) Lateral velocity estimation results.

Fig. 10. Vehicle state estimation results

(a)Vehicle trace: without attitude control

(b) Vehicle trace: with attitude control

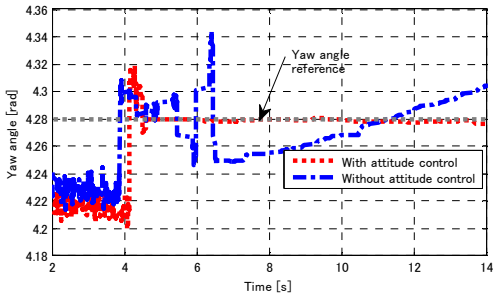

(c) Yaw angle

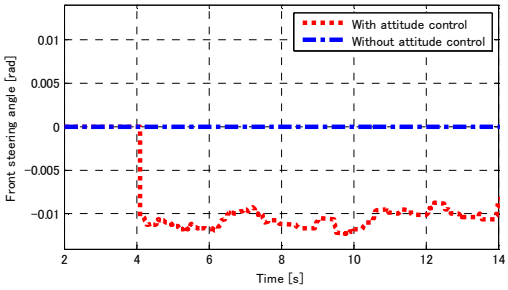

(d) Front steering angle

Fig. 11. Experiment results of attitude control.

yaw rate and lateral acceleration (Aoki *et al.*, 2005). The cornering stiffness of the EV according to road condition in this experiment are $C_f \approx C_r \approx 7000$ [N/rad]. We intentionally design each estimation model with the nominal cornering stiffness $C_{fn} = C_{rn} = 10{,}000$ [N/rad]. This means a considerable model error is introduced to each estimator. Fig. 8 shows that the linear observer using dynamic sensors is sensitive to model error. In contrast, by using the fusion of GPS and gyroscope with proposed Kalman filter algorithm, sideslip angle can be estimated with much smaller estimation error. Results of estimated yaw angle and vehicle attitude measurement are illustrated in Fig. 10 (b). The course angle obtained from GPS receiver is delayed and its sampling time is 200 milliseconds. For comparison, calculated course angle at 1 millisecond is obtained using measured sideslip angle and estimated yaw angle. Using the proposed estimator, the time delay is handled and yaw angle is estimated at high rate (every 1 millisecond).

The estimation results of longitudinal and lateral velocity are shown in Fig. 10 (c) and Fig. 10 (d), respectively. Based on kinematic relationship, a Kalman filter is designed for estimating vehicle velocity (Chen *et al.*, 2008). According to this method, the non-driven wheel's velocity is used as the approximate measurement of EV's longitudinal velocity while longitudinal and lateral accelerations are inputs. Using this method, estimated longitudinal velocity is almost closed to the measured value. However, under the measurement noise and the influence of roll motion to lateral motion, the estimation error of lateral velocity increases considerably. Using the proposed double-layer estimator, the time delay of measurements from GPS receiver is handled, and both longitudinal and lateral velocity are estimated with high accuracy.

5.2 *Verification of Attitude Control*

To evaluate the proposed attitude control, we conduct the autonomous driving test in which the attitude and velocity of EV are automatically controlled by the program.

In case of without attitude control, the front EPS motor always generates zero steering angle for keeping the straight direction of vehicle. However, if the initial position of the steering wheel is not exactly in the mechanic neutral and the initial attitude of the vehicle is not actually the same as the reference values, it is impossible to keep the straight direction of the moving vehicle. Even if the initial attitude and initial position of steering wheel are satisfied, undesirable influence from environment, such as strong lateral wind force, the vehicle cannot follow the desired attitude. Results of the proposed attitude control are shown in Fig. 11 including the vehicle trajectory on Google Earth, yaw angle, and front steering angle command. Front steering angle is generated such that the EV can follow the desired trajectory and yaw angle tracking is assured.

5.3 *Verification of Wheel Slip Ratio Control*

The low friction sheets covered with water were placed on the test course to simulate the slippery road. The desired slip ratio on the slippery road is set as 0.1. Because the vehicle motion was straight in this test, it is necessary to show the results of only one wheel (rear left). The driver accelerated the vehicle with maximum driving command from a starting point close to the low friction sheet. In case of without control, the wheel slip ratio increases considerably on the when entering the slippery road because the motor torque is kept constant as the command from driver (Fig. 12). Fig. 13 shows that with the proposed method, wheel slip ratio tracks the desired value. Thanks to the proposed sliding mode controller, motor torque is controlled to be reduced. Thus, safety traction on low friction road is achieved.

5.4 *Results of Lateral Control*

Cornering tests were conducted on high friction road at the speed of 20 kph. In this test, the steering command was generated by program instead of handling by the driver. Model error of cornering stiffness was introduced to the controller as the experiments of state estimation. As illustrated in Fig. 14 (a) and (b), in case of without control, the responses of the sideslip angle and the yaw rate increase over their reference values. In this case, front steering angle is the same as the driving command. Also, yaw moment is zero which means there is no different torque between rear the left and rear right in-wheel motors. In contrast, with the proposed stability control scheme, front steering angle is generated to be different to the driving command (as shown in Fig. 15 (c)). Yaw moment is also generated by using in-wheel motor torque control (a shown in Fig. 15 (d)). As a result, the controlled variables can track with the reference values, as shown in Fig. 15 (a) and (b). The experimental results confirm that the proposed control system improve the stability of electric vehicle.

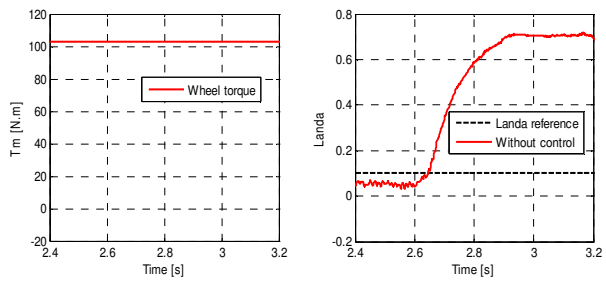

(a) Wheel torque (b) Slip ratio

Fig. 12. EV on slippery road (without control).

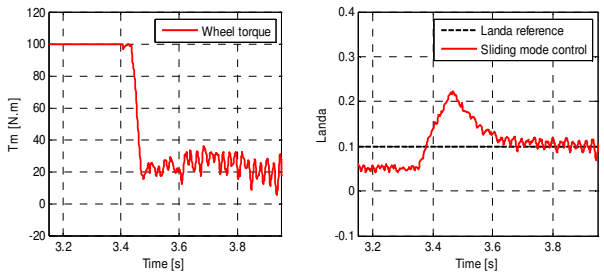

(a) Wheel torque (b) Slip ratio

Fig. 13. EV on slippery road (with traction control).

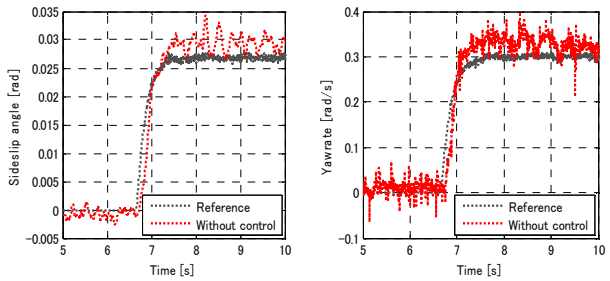

(a) Sideslip angle (b) Yaw rate

Fig. 14. Cornering test (without lateral stability control).

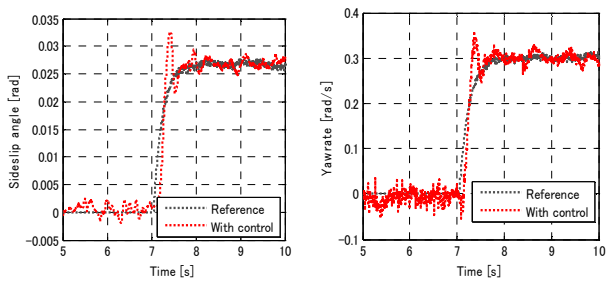

(a) Sideslip angle (b) Yaw rate

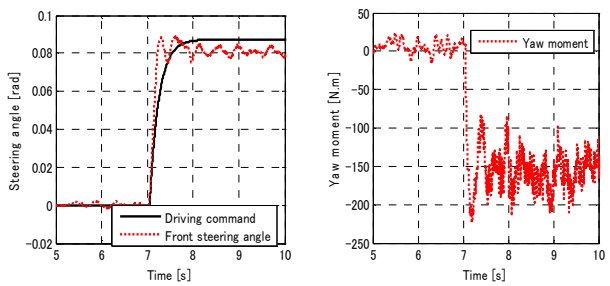

(c) Front steering angle (d) Yaw moment

Fig. 15. Cornering test (with lateral stability control).

6. CONCLUSIONS

We propose a framework of EV motion control based on the integration of single antenna GPS receiver and on-board dynamic sensors. Kalman filter is developed as the core theory of sensor fusion. In order to deal with model uncertainties and external disturbances, disturbance accommodating method is applied in Kalman filter to enhance the robustness of estimation. The time delay of GPS receiver is handled by the reconstruction of measurement in current time applied in Kalman filter. A double-layer state estimator is proposed to provide key states for motion control of EV. Experiments are conducted to verify the effectiveness of the proposal in comparison with other estimation methods using dynamic sensors. Thanks to the state estimator, in this paper, three local motion controls of EV are designed and performed. However, each local controller is evaluated separately from each other. In future works, we will conduct experiments to verify the integration of local motion controllers. The other works will be the design of position estimator and autonomous guidance to complete a framework of autonomous EV considering the stability and safety motion control.

REFERENCES

Anderson, R. and Bevly, D. M. (2004). Estimation of Sideslip Angle Using Model Based Estimator and GPS. *American Control Conference*, Vol. 3, pp. 2122-2127.

Aoki, Y., Uchida, T., and Hori, Y. (2005). Experimental Demonstration of Body Slip Angle Control Based on a Novel Linear Observer for Electric Vehicle. *Annual Conference of the IEEE Industrial Electronics Society*, pp. 2620-2625.

Bevly, D. M., Ryu, J., and Gerdes, J. C. (2006). Integrating INS Sensors with GPS Measurements for Continuous Estimation of Vehicle Sideslip, Roll, and Tire Cornering Stiffness. *IEEE Transactions on Intelligent Transportation System*, Vol. 7, No. 4, pp. 483-493.

Chen, B. C. and Hsieh, F. C. (2008). Sideslip Angle Estimation Using Extended Kalman Filter, *Journal of Vehicle System Dynamics*, Vol. 46, No. 1, pp. 483-493.

Chung, T. and Yi, K. (2006). Design and Evaluation of Sideslip Angle-Based Vehicle Stability Control Scheme on a Virtual Test Track, *IEEE Transactions on Control System Technology*, Vol. 14, No. 2, pp. 224-234.

Daily, R. and Bevly, D. M. (2004). The Use of GPS for Vehicle Stability Control Systems, *IEEE Transactions on Industrial Electronics*, Vol. 51, No. 2, pp. 270-277.

Furukawa, K. and Hori, Y. (2003). Recent Development of Road Condition Estimation Techniques for Electric Vehicle and their Experimental Evaluation using the Test EV "UOT March I and II". *Proceedings of 29th Annual Conference of the IEEE Industrial Electronics Society*, pp. 925-930.

Fujimoto, H. and Yamauchi, Y. (2010). Advanced Motion Control of Electric Vehicle Based on Lateral Force Observer with Active Steering. *Proceedings of IEEE International Symposium on Industrial Electronics*, pp. 3627-2632.

Geng, C., Mostefai, L., Denai, M., and Hori, Y. (2009). Direct Yaw Moment Control of an In Wheel Motored Electric Vehicle Based on Body Slip Angle Fuzzy Observer. *IEEE Transactions on Industrial Electronics*, Vol. 56, pp. 1411-1419.

Hori, Y. (2004). Future Vehicle Driven By Electricity and Control-Research on 4 Wheel Motored UOT March II. *IEEE Transactions on Industrial Electronics*, Vol. 51, No. 5, pp. 954-962.

Hsiao, F. H. and Pan, S. T. (1996). Robust Kalman Filter Synthesis for Uncertain Multiple Time Delay Stochastic Systems. *Journal of Dynamic Systems, Measurement, and Control*, Vol. 118, No. 4, pp. 803-808.

Johnson, C. (1971). Accommodation of External Disturbances in Linear Regulator and Servomechanism Problems. *IEEE Transactions on Automatic Control*, Vol. 16, No. 6, pp. 635-644.

Larsen, T. D., Andersen, N. A., Ravn, O., and Poulsen, N. K. (1998). Incorporation of Time Delayed Measurements in a Discrete-time Kalman Filter. *Proceedings of 37th IEEE Conference on Decision and Control*, pp. 3972-3977.

Nguyen, B. M., Wang, Y., Fujimoto, H., and Hori, Y. (2013a). Electric Vehicle Stability Control Based on Disturbance Accommodating Kalman Filter Using GPS. *Proceedings of IEEE International Conference on Mechatronics*, pp. 382-387.

Nguyen, B. M., Wang, Y., Fujimoto, H., and Hori, Y. (2013b). *Proceedings of 6th IFAC Symposium on Mechatronics System*, pp. 437-444.

Ohnishi, K. (1987). A New Servo Method in Mechatronics. *Transactions of Japanese Society of Electrical Engineers*, 107-D, pp. 83-86.

Suzuki, S. (2012). Autonomous Navigation, Guidance and Control of Small 4-Wheel Electric Vehicle. *Journal of Asian Electric Vehicles*, Vol. 10, No. 1, pp. 1575-1582.

Umeno, T. and Hori, Y. (1991). Robust Speed Control of DC Servomotors Using Modern Two Degrees-of-freedom Controller Design. IEEE Transactions on Industrial Electronics, Vol. 38, No. 5, pp. 363-368.

Yoon, J. H. and Peng, H. (2010). Vehicle Sideslip Angle Estimation Using Two Single Antenna GPS Receivers. *Proceedings of ASME 2010 Dynamic Systems and Control Conference*.

Yoon, J. H. and Peng, H. (2012). Sideslip Angle Estimation Based on GPS and Magnetometer Measurements. *Proceedings of 11th International Symposium on Advanced Vehicle Control*.

Zhao, L. H., Liu, Z. Y., and Chen, H. (2011) Design of a Nonlinear Observer for Vehicle Velocity Estimation and Experiments, *IEEE Transactions on Control Systems Technology*, Vol. 19, No. 3, pp. 664-672.